Published in final edited form as:
Circulation. 2010 August 24; 122(8): 782–789. doi:10.1161/CIRCULATIONAHA.109.935288.

Complex Interactions Between the Sinoatrial Node and Atrium During Reentrant Arrhythmias in the Canine Heart

Vadim V. Fedorov, PhD, **Roger Chang, BSc**, **Alexey V. Glukhov, PhD**, **Geran Kostecki, BSc**, **Deborah Janks, PhD**, **Richard B. Schuessler, PhD**, and **Igor R. Efimov, PhD***

Department of Biomedical Engineering, Washington University, St. Louis, MO, 63130, USA

*Division of Cardiothoracic Surgery, Washington University School of Medicine, St. Louis, MO, 63110, USA

Abstract

Background—Numerous studies implicate the sinoatrial node (SAN) as a participant in atrial arrhythmias, including atrial flutter (AFL) and atrial fibrillation (AF). However, the direct role of the SAN has never been described.

Methods and Results—The SAN was optically mapped in coronary perfused preparations from normal canine hearts (n=17). Optical action potentials (OAPs) were recorded during spontaneous rhythm, overdrive atrial pacing, and AF/AFL induced by Acetylcholine (ACh, 0.3–3 μM) and/or Isoproterenol (Iso, 0.2–1μM). An OAP multiple component algorithm and dominant frequency analysis were used to reconstruct SAN activation and identify specialized sinoatrial conduction pathways (SACPs). Both ACh and Iso facilitated pacing-induced AF/AFL by shortening atrial repolarization. The entire SAN structure created a substrate for macro-reentry with 9.6± 1.7 Hz, n=69 episodes in all preparations. Atrial excitation waves could enter the SAN through the SACPs and overdrive suppress the node. The SACPs acted as a filter for atrial waves by slowing conduction and creating entrance block. ACh/Iso modulated filtering properties of the SACPs by increasing/decreasing the degree of the entrance block, respectively. Thus, the SAN could beat independently from AF/AFl reentrant activity during ACh (49±39%) and ACh/Iso (62±25%) (p=0.38). Without ACh, the AF/AFL waves captured the SAN and overdrive suppressed it. Spontaneous SAN activity could terminate or convert AFL to AF during cholinergic withdrawal.

Conclusions—The specialized structure of the SAN can be a substrate for AF/AFL. Cholinergic stimulation not only can slow sinus rhythm and facilitate AF/AFL, but also protects the intrinsic SAN function from the fast AF/AFL rhythm.

Keywords

Sinoatrial node; optical mapping; acetylcholine; atrial fibrillation; atrial flutter

INTRODUCTION

Both atrial flutter (AFL) and atrial fibrillation (AF) are often associated with sinus node dysfunction.[1–3] Sinoatrial node (SAN) structural and functional abnormalities can play an important role in the initiation and maintenance of AF.[1;2;4–9] On the other hand, the fast

Address for correspondence: Vadim V. Fedorov, Department of Biomedical Engineering, Washington University, Campus Box 1097, One Brookings Drive, St. Louis, Missouri 63130-4899 tel: 1-314-935-6137; fax: 1-314-935-8377; vadimfed@gmail.com.

Disclosures: Authors declare no competitive interests.

AF/AFL rate can lead to SAN dysfunction.[10–12] However, due to the lack of mapping data from the human SAN, no one has directly shown how the SAN participates in AF, nor what the SAN activation is during AF. Do fibrillating waves overdrive suppress the SAN or does the intrinsic SAN activity remain present and even participate in AF?[13] What role does the autonomic nervous system play in the interactions between SAN and AF reentrant waves?[13] While these subjects were widely discussed, no measurements have been published, leaving these questions unanswered until now.[14]

The SAN is a specialized, complex anatomical structure.[15–17] Anatomical[16;18–21] and functional[22;23] studies suggest that the canine SAN is a more realistic model for the human SAN[24;25] than that of small mammals[26;27] (e.g. rabbit and mouse). In both the human and the canine, there are conduction barriers formed by connective tissues surrounding the coronary arteries and SAN tissue, and abrupt changes in Cx43 expression between atrial and nodal cells. Our recent studies [24;25] presented evidence that the canine and human SANs electrically communicate with the atria only through specialized sinoatrial conduction pathways (SACPs). Yet, it is unknown what role the SAN specialized anatomy plays in AFL/AF.

Clinical studies have shown that AF frequently occurs under conditions associated with sympathetic and/or parasympathetic hyperactivity.[28] Autonomic disturbances are also one of the causes of SAN dysfunction.[29–32] Based on these observations, we previously proposed that both cholinergic and adrenergic stimulations can potentiate atrial arrhythmias not only by shortening the atrial refractoriness, but also by inducing pacemaker/conduction abnormalities within the specialized SAN structure.[33] Therefore, this work was designed to study, for the first time, the interactions between the SAN and the atria in the canine model of autonomic-induced AF/AFL using high resolution optical mapping.

METHODS

All animals used (n=17) in this study received humane care in compliance with the National Institutes of Health's Guide for the Care and Use of Laboratory Animals, and the protocol was approved by the Washington University Animal Studies Committee. The isolated perfused canine right atrium[34] as well as the experimental techniques used[27] have been previously described in detail.[25] Optical mapping of the nodal tissues has been described in our previous studies .[25;35;36]

Figure 1A shows an example of the epicardial optical mapping of the canine SAN. The SAN was functionally defined from optical action potential (OAP) morphologies with slow diastolic depolarization and multiple component upstrokes corresponding to asynchronous activation of the SAN tissue layer and atrial layers (Figures 1B–D).[24] This study defined the leading pacemaker as the earliest activation observed within the SAN region (SAN OAP component) and "atrial breakthrough" as the site of earliest activation observed within the atria. Based on our previous study,[24] SACPs were defined as areas of preferential conduction, which correspond to narrow muscular bundles containing both Connexin 43 positive and negative transitional cells between the SAN into larger atrial muscular bundles. SACPs were located between the superior and inferior borders of the SAN and the atria, respectively, and served as conduction bridges between these two structures.

This study used an optimal concentration range of ACh (1.5 ± 0.8 μM) in order to induce sustained AF/AFL episodes without total SAN arrest. If AF/AFl was sustained for more than 10 min, ACh or Iso was transiently washed out, which usually terminated arrhythmias within 1–3 minutes.

To analyze atrial and SAN activations during fast atrial pacing and AF/AFL, a Fast Fourier Transform was applied to determine the dominant frequencies (DF).[37;38] To measure the SAN activation during pacing and atrial reentrant arrhythmias, we used low frequency filters ranging from 10–20 Hz, separating the slow upstroke SAN signals from the fast atria (Online Figures 3 and 4).

For further details, see the Online Data Supplement.

RESULTS

Optical mapping aspects of canine SAN

Figure 1 shows that two distinct activation patterns were observed: the first was SAN excitation from the leading pacemaker and the second was atrial excitation from SACPs[24]. SAN activation map during control (Figure 1E) shows that excitation began in the center of the SAN (OAP #1) and spread inferiorly and superiorly with conduction velocities of 7–16 cm/sec. SAN excitation did not propagate laterally to the CT or medially towards the septum due to the presence of coronary arteries and connective tissue layers as previously described. [24] Atrial breakthrough, (OAP #2), was detected 53 ms after the earliest SAN activation, 6 mm away from the SAN. Thus, the time gap (5–40 ms) in activation between the SAN and atria was likely due to a source-sink mismatch when excitation passes through these narrow SACPs.[39]

Effects of Acetylcholine and Isoproterenol on the SAN automaticity and conduction

In nine preparations, ACh (0.3–3 μM) dose-dependently increased sinus cycle length (SCL) and SAN conduction time (SACT) from 519±22 ms and 54±20 ms to 841±89 ms ($p<0.001$) and 123±40 ms ($p<0.001$), respectively, until rhythm disturbance occurred (a pacemaker shift out of the SAN or exit block). Figures 1C shows that 1 μM ACh slowed sinus rhythm (SR) and nodal conduction, but did not change the atrial activation pattern. However, increasing the dose of ACh depressed conduction mainly in the superior SACP rather than in the inferior SACP (Figure 1E). This switch of preferential conduction to an inferior SACP significantly changed the atrial activation pattern (Figure 1E) and was observed in all preparations during perfusion with ACh (1–3 μM).

Figure 1D shows that 3 μM ACh could induce exit block within the SAN, preventing activation of the atria. This block allowed the SAN OAPs to be detected without atrial signals. SAN exit block was recorded during the perfusion of ACh or during the recovery from ACh effects in 7 of 9 preparations. At higher ACh concentrations (3–10 μM), SAN nodal pacemaker activity was often completely depressed and latent pacemaker activity could be recorded from the inferior (IVC) (n=4) and/or the superior (SVC) vena cavae region (n=2). SAN activity recovered within 1–2 minutes after ACh washout.

In five of the preparations, Iso (1μM) significantly decreased SCL and SACT from 533 ±110 and 54±20 ms to 450±132 ms ($p<0.001$) and 37±18 ms ($p<0.001$). Figure 2 shows an example of the effects of perfusion with Iso on the SAN. During control conditions, the leading pacemaker was located in the inferior SAN and the atria had a bifocal activation pattern. Iso induced a pacemaker shift inside the SAN superiorly from OAP#1 to OAP#3 (Figure 2) and accelerated SR and intranodal conductions. Thus, Iso switched the preferential SACP from an inferior to superior position and changed the atrial activation pattern from bifocal to unifocal (Figure 2C). In two preparations, Iso produced a transient pacemaker shift out of the SAN into the SVC.

ACh also induced a decrease in the action potential duration (APD) of the atrium, but not within the SAN region (Figures 1E, Online Table 1). Iso decreased APD in both the atria and SAN (Figures 2C, Online Table 1).

SAN activity during atrial pacing

Figure 3 demonstrates SAN activation during atrial pacing at a cycle length (CL) of 350 ms. SAN activation began from the left superior anatomical border of the SAN. Thus, this area was defined as the left superior SACP. Excitation from this SACP propagated inferiorly with decrement. No lateral or medial conduction was observed (Figure 3A). During pacing at a CL of 350 ms, there was 1:1 conduction between the atria and the SAN. However, pacing at a CL of 300 ms induced 2:1, Wenckebach-like, entrance block into the SAN (n=10 preparations).

Figures 3B–D show that increasing the pacing rate results in increased SAN entrance block (as large as 4:1) during control conditions. In all DF maps, the SAN stands out as an oval region of lowest frequency (1.5–1.7 Hz), surrounded by the higher frequency atrial region. In control, the frequency of SAN activity was higher during pacing than without pacing: >1.5 Hz vs. 1.45 Hz (SCL=688 ms), which means that SAN was overdrive suppressed by atrial pacing. The SAN was always suppressed during control (n=10) and during the perfusion with Isoproternol (n=5).

A comparison between Figure 3D and Figure 4 shows that perfusion with ACh enhanced entrance block to the SAN (from 4:1 to 7:1). DF and SAN activation maps show that atrial excitation could enter into the SAN only through the inferior SACP, which was a common observation during the perfusion of ACh (n=8). During ACh perfusion, the central SAN region had almost the same rate during pacing and spontaneous SR before pacing: 1.05 Hz vs. 1.07 Hz (SCL=934 ms), indicating that the SAN was not always overdrive suppressed by atrial pacing. Figure 4C demonstrates that the SAN had intrinsic activity during fast pacing due to ACh-induced depression of the conduction through the SACPs.

Effects of ACh and Iso on SAN recovery time

Figure 5A shows the effect of overdrive atrial pacing on SAN recovery time (SANRT) under control conditions and after separate perfusions with ACh (0.3–3 μM) and Iso (0.5–1 μM). Figure 5A represents data obtained only during normal SR before and after pacing. ACh consistently prolonged the corrected SANRT from 131±31 to 199±45 ms ($p<0.001$) while beta-adrenergic stimulation with Iso decreased the corrected SANRT to 64±59 ms ($p<0.001$), consistent with previous observations by Chadda et al[40] (Figure 5B).

Figure 5B separately presents SANRT data for all cases (15 cases from 9 different preparations) of pacing induced SAN exit block observed during perfusion with ACh (0.3 to 3 μM). Figure 5C shows an example of SAN exit block induced during pacing. SAN exit block resulted from conduction failure within SACP(s) promoted by both pacing and ACh. In all cases of exit block, there was no significant difference in SCL before or after pacing: 883±82 vs 841±89 ms ($p>0.05$). These findings support the observation shown in Figure 4C that ACh-induced bidirectional block within the SACP can prevent SAN from overdrive suppression by pacing. Iso (n=3) or Atropine (3μM, n= 3) recovered ACh-induced and pacing-induced SAN exit blocks (see Online Figure 5).

SAN activity during sustained AF/AFL

Under control conditions, only one episode of sustained AFL was induced by atrial pacing (Figure 6A). However, in preparations with ACh (4.8 ± 3.9 μM) (n=10), Iso (1 μM) (n=2),

and mixtures of ACh (1μM) and Iso (0.2–1 μM) (n=3), atrial pacing induced multiple episodes of sustained AFL and AF (>3 min) (Figures 6–7; Online Figures 1–2).

The mechanism of sustained AFL (26 episodes from 10 preparations) was consistently observed to be macro-reentrant excitation around the SAN, which functioned as a conduction barrier (Figure 6, Online Figures 1–2). Figure 6A demonstrates that under control conditions, AFL could overdrive suppress the SAN through the SACPs, causing 3:1 – 4:1 entrance block into the SAN (Online Movie 1). Iso alone could induce sustained AFL (n = 2), but not AF. Iso-induced reentry activated the SAN from both the superior and inferior pathways with entrance block (4:1) (Figure 6B). The perfusion of ACh during atrial pacing induced AFL in 8 out of 10 preparations with CL 97±25 ms (10.2±3.5 Hz). ACh prevented overdrive suppression of the SAN by inducing entrance block into the SAN (up to 11:1), permitting intrinsic SAN pacemaker activity. The SAN activation map in Figure 6C demonstrates the presence of intrinsic SAN pacemaker activity during ACh-induced AFL (Online Movie 2).

Usually, ACh sustained AFL, but during ACh washout, AFL converted to AF (Figure 6D) and preserved the SAN intrinsic pacemaker activity. Before ACh washout terminated AF/AFL, SAN activity significantly accelerated from 1.18±0.36 Hz to 1.63±0.33 Hz ($p<0.01$, n=10). There were several recorded cases from three different preparations that demonstrated the conversion from AFL to AF and AF to AFL. During ACh-induced entrance block, the SAN wave activated the atrium and interacted with the reentrant wavefront to terminate reentry or convert AFL to AF (Online Movie 2).

ACh-induced AF (47 episodes from 10 preparations) was usually associated with reentrant excitations around the pectinate muscles and/or SVC and IVC regions with a maximum DF of 22.32± 5.86 Hz and atrial DF around the SAN of 11.26 ± 5.23 Hz (Figure 7, Online Table 2). Figure 7A and 7B illustrate that AF episodes induced during the perfusion of a mixture of ACh and Iso had a higher frequency of SAN activity than during the perfusion of ACh only (1.64±0.22 Hz vs. 1.17±0.21 Hz, $p<0.01$ n=6) (Figure 7). Figure 7C and 7D show an example of three possible interactions observed between the atria and the SAN: (1) intrinsic SAN pacemaker activity, which escapes into the atria; (2) entrance block in the SACPs, leaving the intrinsic SAN pacemaker activity intact; (3) both exit and entrance block in the SACPs. These various scenarios occurred in random order. The percentages of total recorded SAN beats that were not paced by the atria during ACh-induced and ACh/Iso-induced AF/AFL were 49±39% and 62±25%, respectively. The frequency of the SAN activities during all analyzed episodes of AF/AFL was close to the control SR values before or after the arrhythmia (1.38±0.51 vs. 1.30±0.31 Hz, p= 0.65).

DISCUSSION

Canine model of the interactions between the SAN and atria

Figure 8 shows a 3D structural model of the canine SAN and region of atria mapped, (modified from Fedorov et al[24]) summarizing the principal findings of this study. By using ACh and Iso as well as atrial pacing, the present study found functional evidence for at least four SACPs. The main new findings from our present study are:

1. Atrial excitation waves can enter into the SAN through the SACPs and overdrive suppresses the node. The SACPs act like a low pass filter for atrial waves by slowing conduction and creating entrance block.
2. ACh and Iso modulate these filtering properties of the SACPs by increasing or decreasing the degree of the entrance block, respectively.

3. Conduction properties of the superior SACPs have a higher sensitivity to autonomic stimulation than the inferior SACPs.
4. The entire SAN structure creates a substrate for macro-reentry (typical AFL).
5. During cholinergic stimulation, the SAN can beat independently from AF/AFl reentrant activity. During control and with Iso, the AF/AFL waves capture the SAN and overdrive suppress it.
6. Spontaneous SAN activity can terminate or convert AFL to AF during cholinergic withdrawal.

Effects of sympathetic and parasympathetic stimulation on SAN function

In the present study, perfusion with Iso and ACh generally resulted in a preferential use of superior and inferior SACPs, respectively, due to a shift in the location of the leading pacemaker and/or inhomogeneous changes in conduction within SAN (Figure 8D and Figures 1–2). We propose that the inferior and superior SACPs have different conduction properties and different sensitivities to ACh and Iso due to spatial differences in muscarinic and beta-adrenergic receptors.[41] The distance of the pacemaker shift inside the SAN varies from 1 to 15 mm (Figures 1E and 2C). However, even with a negligible pacemaker shift there are changes in the preferential SACP due to inhomogeneous conduction changes within the SAN (Figure 1E). Thus, the atrial breakthrough site can be moved by drugs even more, up to 25 mm, without significant shift of the leading pacemaker inside of the SAN. These results provide an explanation of the previous canine studies[34;42;43], which demonstrated that sympathetic stimulation accelerated SR and superiorly shifted the area of earliest atrial activation, but cholinergic stimulation slowed SR and inferiorly shifted the breakthrough site 10–20 mm away.

In addition, ACh can depress conduction in all of the SACPs – resulting in SAN exit block (Figure 8E, Figures 1 and 3) – or induce SAN inexcitability (Figure 8F).[44] Under these conditions, the present study observed pacemaker shifts into the IVC or SVC regions (Figure 1D). Iso can also accelerate these or other latent pacemakers and cause transient pacemaker shift outside of the SAN.

The study shows that slow atrial pacing (350–400 ms) preferentially conducts through the left superior SACP (Figure 3A and Figure 8C) and that faster pacing rates (CL<300 ms) and ACh cause preferentially conduction through the inferior SACPs (Figure 4 and Figure 8C, 8D).

SAN role in AF/AFL mechanisms

In their classical microelectrode study of the rabbit SAN, Kirchhof and Allessie discovered a high degree of SAN entrance block (5:1) during low potassium-induced AF.[13] However, it is uncertain whether or not the conclusions made from small animal models (e.g. rabbit) about the function of the SAN during AF/AFL are the same as in large, more complex 3D structures such as canine[24] and human SANs.[3;25] Neither Kirchhof and Allessie[45] nor any other studies directly demonstrated how the SAN functionally and structurally participates in atrial reentrant arrhythmias.

The present study for the first time demonstrated that the SAN structure is a substrate for macroreentry. Sustained AFL reentry circuit under all conditions (control, ACh and Iso) tend to anchor around the SAN structure (see Figure 6), as was observed in a previous rabbit study.[27] Our recent optical mapping studies confirm that the human SAN structure could also be a substrate for the typical AFL mechanism in humans.[25] In the present study, AF is

maintained by a single or multiple reentry circuits anchored mostly to the pectinate muscles as previously demonstrated (Figures 7–8, Online Figure 6). [46–48]

The present study demonstrated that SACPs play a major role in creating SAN entrance blocks during atrial pacing (see Figure 4), AFL (see Figure 6), or AF (see Figure 7). ACh can promote conduction block in the SACP and thus prevent AF/AFl impulses from suppressing the intrinsic SAN activity. Some SAN impulses can escape through these SACPs during AF/AFL and partially activate the surrounding atria during washout from ACh (Figure 6D) or during the addition of Iso (Figure 7D). Thus, SAN impulses might perpetuate the arrhythmogenic process (Figure 6D, Online Movie 2). In the present canine model, AF can be converted to AFL and back to AF or to SR during washout from ACh. The SAN can also participate in these conversions due to faster recovery of pacemaker activity and conduction in the SACPs (Figures 6D, 8J and 8K). Moreover, the present study's observation of accelerated SAN activity during AF induced by a mixture of ACh and Iso (Figure 7) can explain our previous observation as to how Iso potentiates the initiation and maintenance of ACh- mediated AF.[33]

Potential Implications

Disturbances in the autonomic nervous system can be a cause of both SAN dysfunctions[8;29] and paroxysmal AF/AFL.[28] Thus, the cholinergic induced SAN dysfunctions (exit blocks, and depressed intranodal conduction and automaticity) make the canine model of AF clinically relevant. Moreover, parasympathetic stimulation can also preserve the SAN function from the fast AF rate by enhancing the filtering properties of the SACP, resulting in entrance block. Thus, it can prevent overdrive pacing induced remodeling of the SAN during atrial tachycardias.[12] We propose that the present comprehensive study of the interaction between the SAN and atria will help to explain the role of an increased/reduced sympathetic and vagal tone in patients with early AF recurrence[49] and suggest how autonomic control may contribute to the initiation and maintenance of AF/AFL.

CONCLUSION

This study demonstrates that the SACPs play an important role in the protection of the SAN against overdrive pacing from AF/AFL. However, the specialized functional structure of the SAN can be a substrate for both the initiation and maintenance of AF/AFL.

Supplementary Material

Refer to Web version on PubMed Central for supplementary material.

Acknowledgments

The authors thank Dr. Stanislav Zakharkin for help in statistical analysis of the data.

Sources of Funding: The project was supported by the American Heart Association Beginning Grant In Aid 0860047Z (VVF), NIH RO1 HL0322257 and RO1 HL085113 (RBS), NIH R01 HL085369 and RO1 HL067322 (IRE).

LIST OF ABBREVIATIONS

ACh	acetylcholine
AF	atrial fibrillation
AFL	atrial flutter

APD	action potential duration
CT	crista terminalis
DF	dominant frequency
IAS	intratrial septum
Iso	isoproterenol
IVC	inferior vena cava
OAP	optical action potential
RAA	right atrial appendage
SAN	sinoatrial node
SACT	sinoatrial conduction time
SANRT	SAN recovery time
SACP	sinoatrial conduction pathways
SCL	sinus cycle length
SR	sinus rhythm
SVC	superior vena cava

Reference List

1. Birchfield R, Menefee E, Bryant G. Disease of the sinoatrial node associated with bradycardia, asystole, syncope, and paroxysmal atrial fibrillation. Circulation. 1957; 16:20–26. [PubMed: 13447146]
2. Gomes JA, Kang PS, Matheson M, Gough WB Jr, El Sherif N. Coexistence of sick sinus rhythm and atrial flutter-fibrillation. Circulation. 1981; 63:80–86. [PubMed: 7438410]
3. Schuessler RB. Abnormal sinus node function in clinical arrhythmias. J Cardiovasc Electrophysiol. 2003; 14:215–217. [PubMed: 12693509]
4. Nadeau RA, Roberge FA, Billette J. Role of the sinus node in the mechanism of cholinergic atrial fibrillation. Circ Res. 1970; 27:129–138. [PubMed: 5424562]
5. Sanders P, Morton JB, Kistler PM, Spence SJ, Davidson NC, Hussin A, Vohra JK, Sparks PB, Kalman JM. Electrophysiological and electroanatomic characterization of the atria in sinus node disease: evidence of diffuse atrial remodeling. Circulation. 2004; 109:1514–1522. [PubMed: 15007004]
6. Wu DL, Yeh SJ, Lin FC, Wang CC, Cherng WJ. Sinus automaticity and sinoatrial conduction in severe symptomatic sick sinus syndrome. J Am Coll Cardiol. 1992; 19:355–364. [PubMed: 1732365]
7. Gomes JA, Kang PS, El Sherif N. The sinus node electrogram in patients with and without sick sinus syndrome: techniques and correlation between directly measured and indirectly estimated sinoatrial conduction time. Circulation. 1982; 66:864–873. [PubMed: 7116602]
8. Mandel WJ, Jordan JL, Karagueuzian HS. Disorders of Sinus Function. Curr Treat Options Cardiovasc Med. 1999; 1:179–186. [PubMed: 11096482]
9. Takahashi Y, Sanders P, Rotter M, Rostock T, Haissaguerre M. Sinus node region as an ultimate source driving chronic atrial fibrillation. J Cardiovasc Electrophysiol. 2005; 16:1023. [PubMed: 16174027]
10. Elvan A, Wylie K, Zipes DP. Pacing-induced chronic atrial fibrillation impairs sinus node function in dogs. Electrophysiological remodeling. Circulation. 1996; 94:2953–2960. [PubMed: 8941126]

11. Sparks PB, Jayaprakash S, Vohra JK, Kalman JM. Electrical remodeling of the atria associated with paroxysmal and chronic atrial flutter. Circulation. 2000; 102:1807–1813. [PubMed: 11023936]
12. Yeh YH, Burstein B, Qi XY, Sakabe M, Chartier D, Comtois P, Wang Z, Kuo CT, Nattel S. Funny current downregulation and sinus node dysfunction associated with atrial tachyarrhythmia: a molecular basis for tachycardia-bradycardia syndrome. Circulation. 2009; 119:1576–1585. [PubMed: 19289641]
13. Kirchhof CJ, Allessie MA. Sinus node automaticity during atrial fibrillation in isolated rabbit hearts. Circulation. 1992; 86:263–71. [PubMed: 1344190]
14. Page PL. Sinus node during atrial fibrillation. To beat or not to beat? Circulation. 1992; 86:334–336. [PubMed: 1617785]
15. Keith A, Flack M. The form and nature of the muscular connection between the primary divisions of the vertebrate heart. J Anat Physiol. 1907; 41:172–189. [PubMed: 17232727]
16. James TN. Anatomy of the human sinus node. Anat Rec. 1961; 141:109–139. [PubMed: 14451023]
17. James TN. Structure and function of the sinus node, AV node and His bundle of the human heart: part I-structure. Prog Cardiovasc Dis. 2002; 45:235–267. [PubMed: 12525999]
18. James TN, Sherf L, Fine G, Morales AR. Comparative ultrastructure of the sinus node in man and dog. Circulation. 1966; 34:139–163. [PubMed: 5942665]
19. Truex RC, Smythe MQ. Comparative morphology of the cardiac conduction tissue in animals. Ann N Y Acad Sci. 1965; 127:19–33. [PubMed: 5217260]
20. Truex RC, Smythe MQ, Taylor MJ. Reconstruction of the human sinoatrial node. Anat Rec. 1967; 159:371–378. [PubMed: 5586287]
21. Bromberg BI, Hand DE, Schuessler RB, Boineau JP. Primary negativity does not predict dominant pacemaker location: implications for sinoatrial conduction. Am J Physiol. 1995; 269:H877–H887. [PubMed: 7573531]
22. Schuessler RB, Boineau JP, Wylds AC, Hill DA, Miller CB, Roeske WR. Effect of canine cardiac nerves on heart rate, rhythm, and pacemaker location. Am J Physiol. 1986; 250:H630–H644. [PubMed: 3963219]
23. Boineau JP, Canavan TE, Schuessler RB, Cain ME, Corr PB, Cox JL. Demonstration of a widely distributed atrial pacemaker complex in the human heart. Circulation. 1988; 77:1221–1237. [PubMed: 3370764]
24. Fedorov VV, Schuessler RB, Hemphill M, Ambrosi CM, Chang R, Voloshina AS, Brown K, Hucker WJ, Efimov IR. Structural and functional evidence for discrete exit pathways that connect the canine sinoatrial node and atria. Circ Res. 2009; 104:915–923. [PubMed: 19246679]
25. Fedorov VV, Glukhov AV, Chang R, Kostecki G, Alferol H, Wuskell J, Loew LM, Moazami N, Efimov IR. The origin of heartbeat in the human sinus node: evidence of sino-atrial exit pathways. Circulation. 2009; 120:S673–S674.
26. Boyett MR, Honjo H, Kodama I. The sinoatrial node, a heterogeneous pacemaker structure. Cardiovasc Res. 2000; 47:658–687. [PubMed: 10974216]
27. Fedorov VV, Hucker WJ, Dobrzynski H, Rosenshtraukh LV, Efimov IR. Postganglionic Nerve Stimulation Induces Temporal Inhibition of Excitability in the Rabbit Sinoatrial Node. Am J Physiol. 2006; 291:H612–H623.
28. Coumel P. Paroxysmal atrial fibrillation: role of autonomic nervous system. Arch Mal Coeur Vaiss. 1994; 87(Spec No 3):55–62. [PubMed: 7786125]
29. Kerin NZ, Louridas G, Edelstein J, Levy MN. Interactions among the critical factors affecting sinus node function: the quantitative effects of the duration and frequency of atrial pacing and of vagal and sympathetic stimulation upon overdrive suppression of the sinus node. Am Heart J. 1983; 105:215–223. [PubMed: 6823801]
30. Levy MN. Sympathetic-vagal interactions in the sinus and atrioventricular nodes. Prog Clin Biol Res. 1988; 275:187–197. [PubMed: 3051009]
31. Kuga K, Yamaguchi I, Sugishita Y, Ito I. Assessment by autonomic blockade of age-related changes of the sinus node function and autonomic regulation in sick sinus syndrome. Am J Cardiol. 1988; 61:361–366. [PubMed: 3341215]

32. Kang PS, Gomes JA, Kelen G, El Sherif N. Role of autonomic regulatory mechanism in sinoatrial conduction and sinus node automaticity in sick sinus syndrome. Circulation. 1981; 64:832–838. [PubMed: 7273383]
33. Sharifov OF, Fedorov VV, Beloshapko GG, Glukhov AV, Yushmanova AV, Rosenshtraukh LV. Roles of adrenergic and cholinergic stimulation in spontaneous atrial fibrillation in dogs. J Am Coll Cardiol. 2004; 43:483–490. [PubMed: 15013134]
34. Schuessler RB, Bromberg BI, Boineau JP. Effect of neurotransmitters on the activation sequence of the isolated atrium. Am J Physiol. 1990; 258:H1632–H1641. [PubMed: 1972866]
35. Efimov IR, Fedorov VV, Joung B, Lin SF. Mapping cardiac pacemaker circuits: methodological puzzles of the sinoatrial node optical mapping. Circ Res. 2010; 106:255–271. [PubMed: 20133911]
36. Efimov IR, Mazgalev TN. High-resolution three-dimensional fluorescent imaging reveals multilayer conduction pattern in the atrioventricular node. Circulation. 1998; 98:54–57. [PubMed: 9665060]
37. Mandapati R, Skanes A, Chen J, Berenfeld O, Jalife J. Stable microreentrant sources as a mechanism of atrial fibrillation in the isolated sheep heart. Circulation. 2000; 101:194–199. [PubMed: 10637208]
38. Bagwe S, Berenfeld O, Vaidya D, Morley GE, Jalife J. Altered right atrial excitation and propagation in connexin40 knockout mice. Circulation. 2005; 112:2245–2253. [PubMed: 16203917]
39. Rohr S, Kucera JP, Fast VG, Kleber AG. Paradoxical Improvement of Impulse Conduction in Cardiac Tissue by Partial Cellular Uncoupling. Science. 1997; 275:841–844. [PubMed: 9012353]
40. Chadda KD, Banka VS, Bodenheimer MM, Helfant RH. Corrected sinus node recovery time. Experimental physiologic and pathologic determinants. Circulation. 1975; 51:797–801. [PubMed: 1122582]
41. Beau SL, Hand DE, Schuessler RB, Bromberg BI, Kwon B, Boineau JP, Saffitz JE. Relative densities of muscarinic cholinergic and beta-adrenergic receptors in the canine sinoatrial node and their relation to sites of pacemaker activity. Circ Res. 1995; 77:957–963. [PubMed: 7554150]
42. Meek WJ, Eyster JAE. The effect of vagal stimulation and of colling on the location of the pacemaker within the sino-auricular node. Am J Physiol. 1914; 34:368–383.
43. Schuessler RB, Boineau JP, Wylds AC, Hill DA, Miller CB, Roeske WR. Effect of canine cardiac nerves on heart rate, rhythm, and pacemaker location. Am J Physiol. 1986; 250:H630–H644. [PubMed: 3963219]
44. Vinogradova TM, Fedorov VV, Yuzyuk TN, Zaitsev AV, Rosenshtraukh LV. Local cholinergic suppression of pacemaker activity in the rabbit sinoatrial node. J Cardiovasc Pharmacol. 1998; 32:413–424. [PubMed: 9733355]
45. Allessie MA, Bonke FI. Direct demonstration of sinus node reentry in the rabbit heart. Circ Res. 1979; 44:557–68. [PubMed: 428051]
46. Schuessler RB, Grayson TM, Bromberg BI, Cox JL, Boineau JP. Cholinergically mediated tachyarrhythmias induced by a single extrastimulus in the isolated canine right atrium. Circ Res. 1992; 71:1254–1267. [PubMed: 1394883]
47. Berenfeld O, Zaitsev AV, Mironov SF, Pertsov AM, Jalife J. Frequency-dependent breakdown of wave propagation into fibrillatory conduction across the pectinate muscle network in the isolated sheep right atrium. Circ Res. 2002; 90:1173–1180. [PubMed: 12065320]
48. Allessie, MA.; Lammers, WJEP.; Bonke, FIM.; Hollen, J. Experimental evaluation of Moe's multiple wavelet hypothesis of atrial fibrillation. In: Zipes, DP.; Jalife, J., editors. Cardiac Electrophysiology and Arrhythmias. Grune & Stratton; Orlando: 1985.
49. Lombardi F, Colombo A, Basilico B, Ravaglia R, Garbin M, Vergani D, Battezzati PM, Fiorentini C. Heart rate variability and early recurrence of atrial fibrillation after electrical cardioversion. J Am Coll Cardiol. 2001; 37:157–162. [PubMed: 11153731]

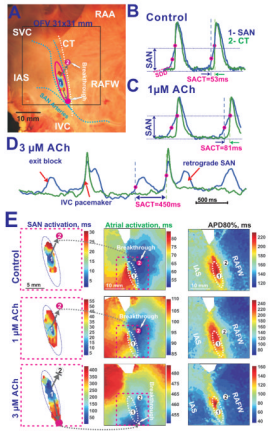

Figure 1. ACh effects on the canine SAN preparation during slowing sinus rhythm

Panel A – Image of the canine preparation that depicts the location of the SAN (pink oval), SAN activation, optical field of view (OFV) (black box), and coronary arteries (dotted blue lines). In all panels, the beginning of the atrial activation sequence (breakthrough) is signified by pink circles. Grey arrows indicate sinoatrial exit pathways (SACPs).

Panels B, C and D - OAPs in control conditions and during perfusion with 1 μM and 3 μM Ach, respectively. The SAN OAP (blue #1) was chosen from the center of the SAN (1). The atrial OAP (green #2) represents the earliest atrial excitation site in the CT. Optical recordings from the SAN exhibit the slow diastolic depolarization (SDD), slowly rising upstroke of the SAN (SAN component) and the rapidly rising upstroke of the atrial myocardium (atrial component).

Panel E– Separated SAN and atrial activation maps as well as action potential duration (APD80%) maps during control and during perfusion with 1 μM and 3 μM ACh. The unlabeled, dotted ovals show the approximate border of the SAN region. The pink dotted squares show enlarged views of the SAN activation maps.

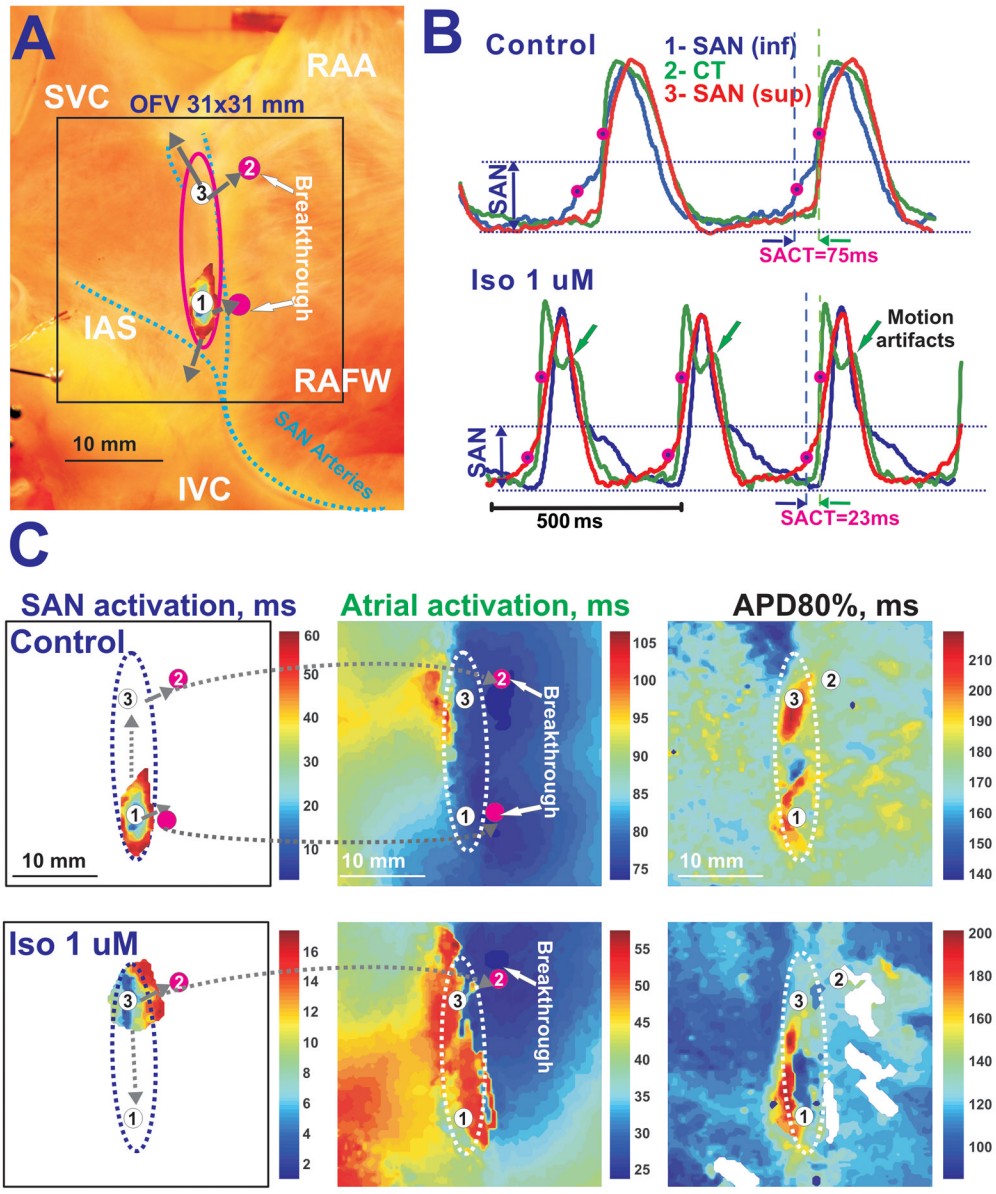

Figure 2. Iso effects on the canine SAN preparation during sinus rhythm

Panel A – Image of the canine SAN preparation. Denotations are the same as in Figure 1.

Panel B - The effect of Iso on shortening CL and SACT. OAPs taken from the inferior SAN leading pacemaker in control (1-blue), the earliest atrial excitation site in the crista terminalis CT (2-green), and the superior SAN leading pacemaker during Iso (3-red) during control conditions and perfusion with 1 μM Iso.

Panel C – Separated SAN and atrial activation maps with corresponding action potential duration (APD80%) maps in control and during Iso perfusion.

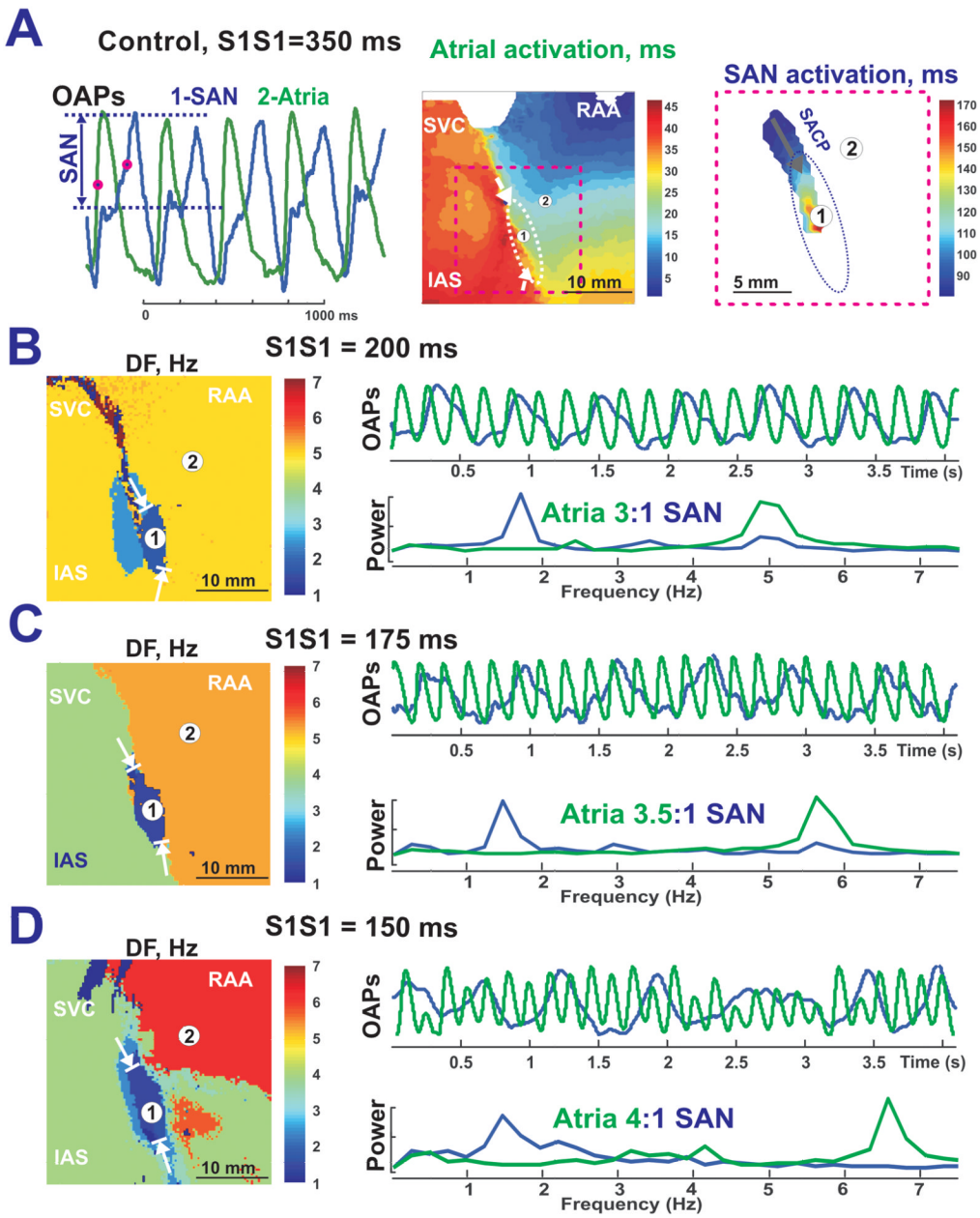

Figure 3. SAN activity during atrial pacing in control

Panel A – OAPs from SAN (blue #1) and atrial myocardium (green #2), and separated atrial and SAN activation maps during atrial pacing at 350 ms. Arrows in the color maps show functional SACPs during pacing (same preparation as Figure 1).

Panel B, C and D - DF maps of epicardial OAPs recorded during increased pacing rates under control conditions. The selected SAN OAP (blue #1) and atrial OAP (green #2) with the associated power spectrum are shown beside each corresponding DF map.

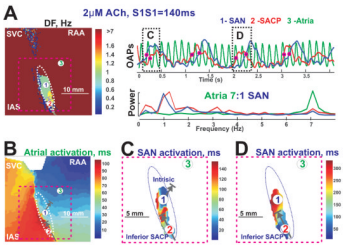

Figure 4. SAN activation during fast atrial pacing and 2 μM ACh

Panel A - A dominant Frequency map of epicardial OAPs recorded during atrial pacing at a CL of 140 ms with 2 μM Ach along with OAPs and their frequency power spectrums selected from the SAN center (blue #1), inferior SAN (red #2) and right atrial free wall (green #3). Arrows in the color maps show functional SACPs during pacing.

Panel B - Atrial activation map.

Panel C and **D** – enlarged views of SAN activations corresponding to the OAPs shown in **Panel A**, indicated by pink dashed lines.

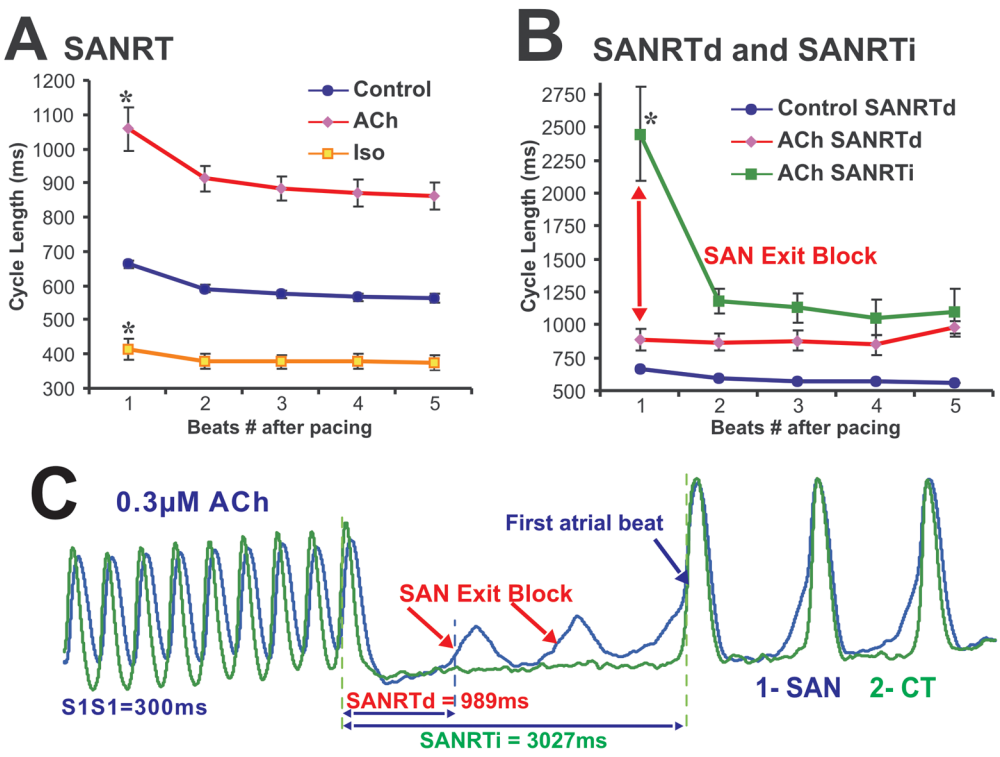

Figure 5. SAN recovery time in control and after ACh and Iso perfusion

Panels A – SANRT during control conditions and during perfusion with ACh and Iso.

Panel B - SANRTd (direct) and SANRTi (indirect) for pacing-induced SAN exit block cases during perfusion with ACh.

Panel C – An example of SANRTd and SANRTi measurements taken during an episode of exit block, which occurred during perfusion with ACh. SAN OAP shown was selected from the center of the SAN while the atrial OAP was selected from the CT.

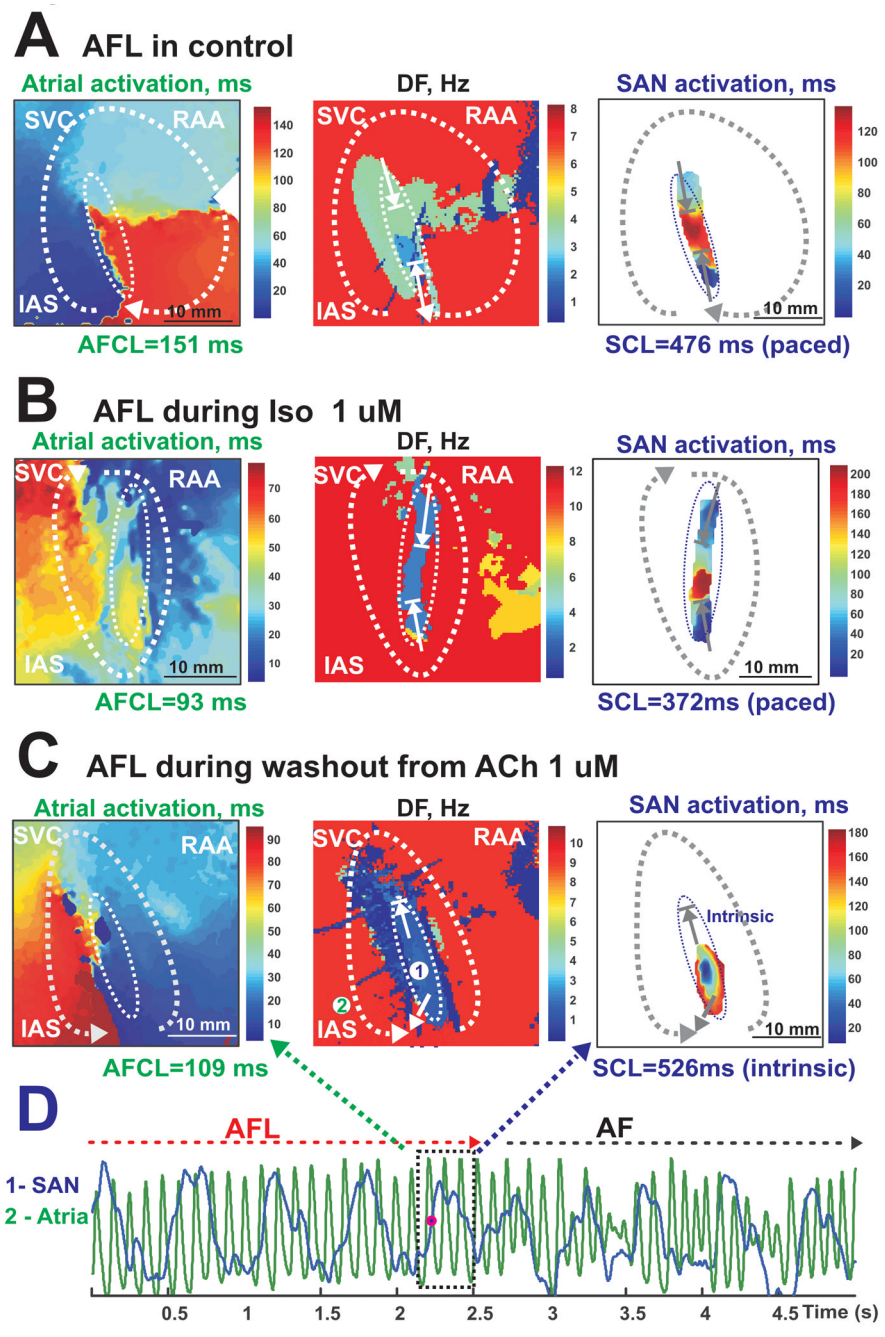

Figure 6. SAN activation during AFL in control, ACh and Iso perfusions

Panels A, B, and C show atrial activation maps, DF maps and examples of SAN activation during different AFL episodes. All of the atrial activation maps clearly show a single macroreentrant circuit of AFL (dotted white arrow) around the SAN structure.

Panels A and B are from the same preparation.

Panel A - The interaction between the SAN and the atria during control AFL.

Panel B - The interaction between the SAN and the atria during Iso-induced AFL. The SAN activation map shows no intrinsic pacemaker activity.

Panel C - The interaction between the SAN and the atria during ACh (1 μM) washout. Unlike control (**Panel A**) or Iso (**Panel B**) conditions, the SAN had its own intrinsic pacemaker activity as depicted in the SAN activation and DF maps.
Panel D - Conversion of AFL (**Panel C**) to AF during washout from ACh.

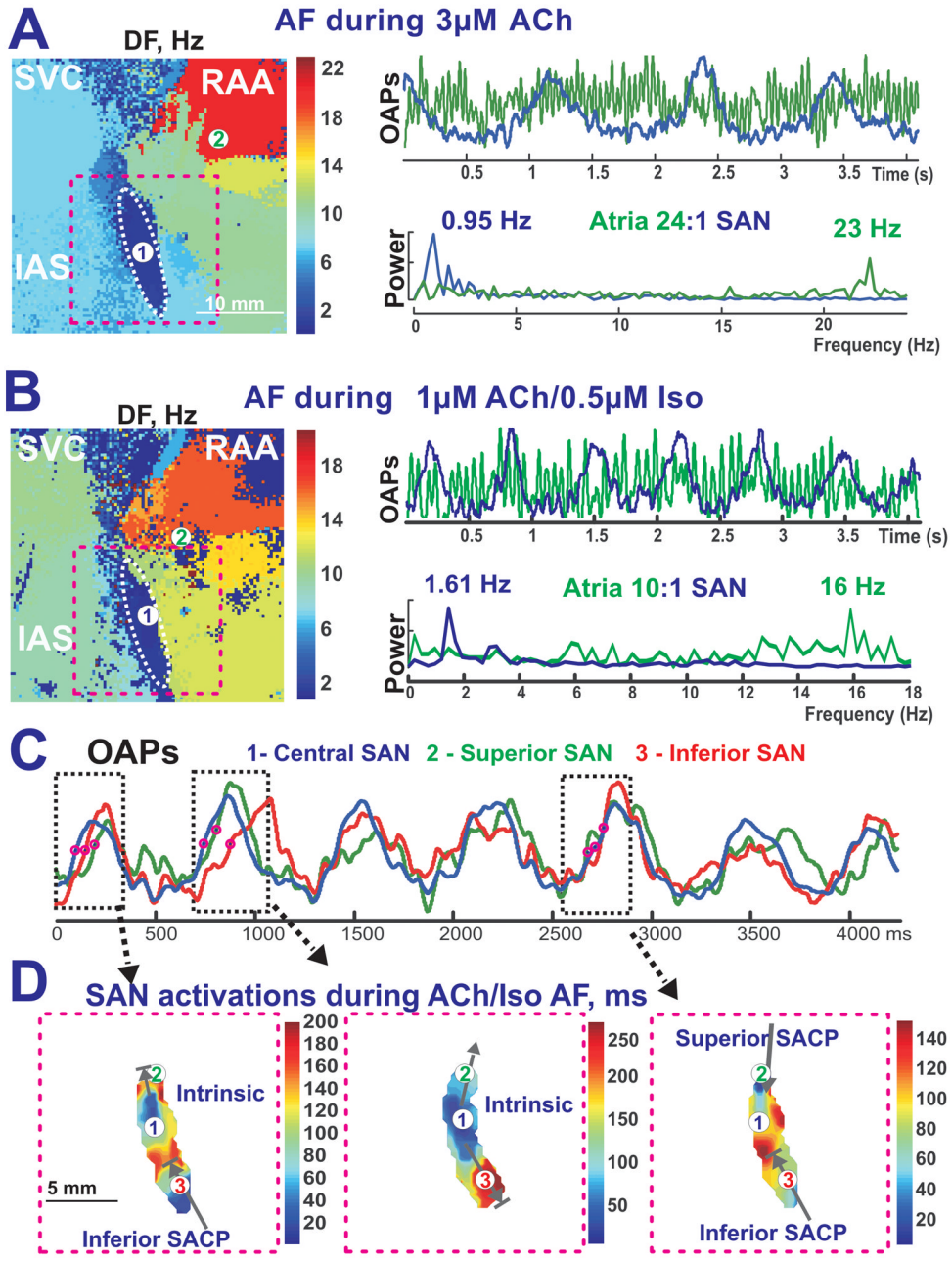

Figure 7. The complex interaction between reentrant atrial waves and SAN intrinsic activity during sustained ACh-induced AF and ACh/Iso-induced AF

Panels A and B – The complicated interaction between the atria and the SAN during sustained ACh (3 μM)-induced AF (**Panel A**) and sustained ACh (1 μM) and Iso (0.5 μM)-induced AF (**Panel B**) (same preparation as Figure 1). The left panels show DF maps, while the right panels show the SAN and atrial OAP recordings and the corresponding frequency power spectrum.

Panel C - OAP recording during ACh/Iso induced AF (**panel B**) from the SAN region broken up into three components: Central SAN (blue #1), Superior SACP (green #2), and Inferior SACP (red #3).

Panel D - Enlarged views of the SAN activation map (pink dotted rectangle in **Panel A**) during times shown by black dotted rectangle in **Panel C**.

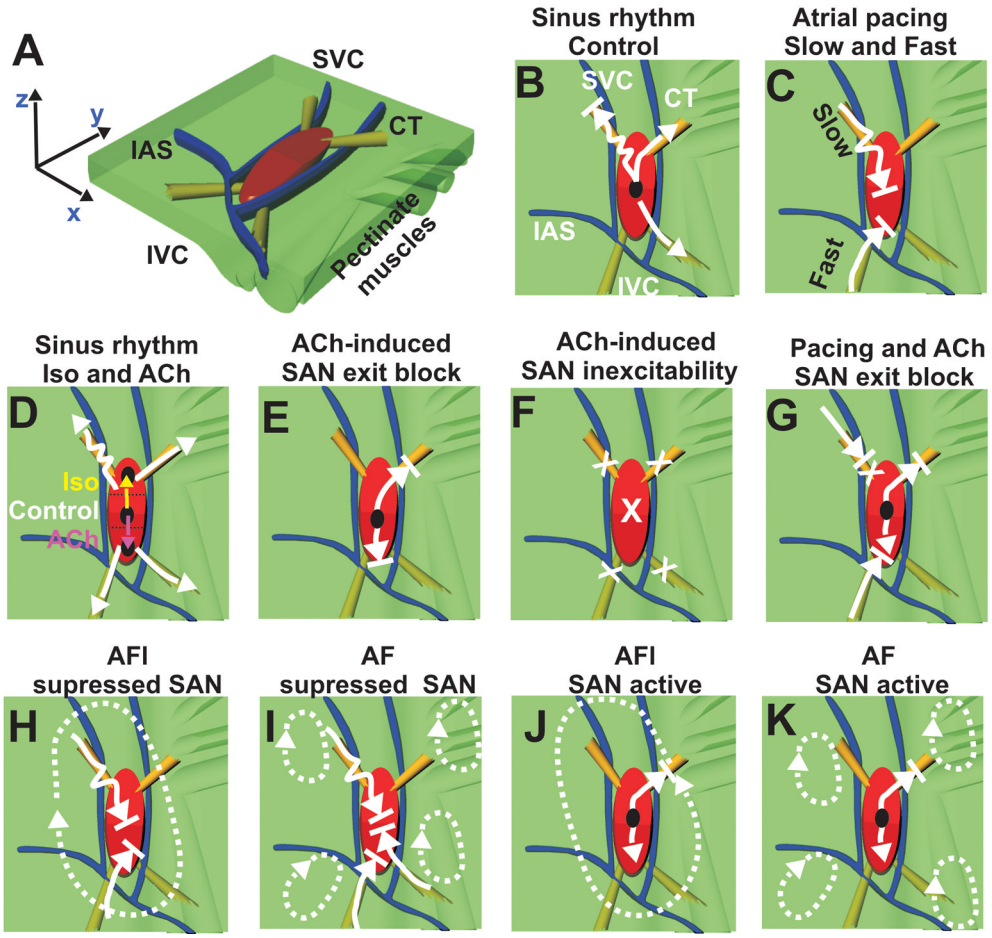

Figure 8. The canine SAN model: SAN activity during normal SR, atrial pacing and reentrant arrhythmias

Panel A - Perspective, epicardial view of the canine SAN model with the orientation and location of the pectinate muscles (green bundles) defined. A 3D model of the SAN based on the functional and structural data was created using the Rhinoceros 3D software (McNeel). The atrial myocardium (green) and the three bifurcating coronary arteries (blue) surround the SAN (red). The yellow bundles show the SACPs.

The remaining panels (**Panels B–K**) were observations from the optical recordings overlaid on an epicardial view of the model with the same anatomical orientation. Black circles show leading pacemaker sites inside or outside of the SAN. The white arrows show the preferential directions of the excitation propagation through SAN pathways. Squiggled arrows represent conduction with decrement. Arrows with a line at the tip represent blocked conduction. X's represent complete inhibition. Dotted white arrows show AF/AFL reentrant circuits.